The Activity of Selected RB69 DNA Polymerase Mutants Can Be Restored by Manganese Ions: The Existence of Alternative Metal Ion Ligands Used during the Polymerization Cycle†

E. Zakharova, J. Wang, and W. Konigsberg*

Department of Molecular Biophysics and Biochemistry, Yale University, 333 Cedar Street, New Haven, Connecticut 06520

Received February 24, 2004; Revised Manuscript Received March 30, 2004

ABSTRACT: Site specific mutants in the pol active center of RB69 DNA polymerase have been produced and studied using rapid chemical-quench techniques. Pre-steady-state kinetic analysis carried out with Mg^{2+} and Mn^{2+} has enabled us to divide the mutants into two groups. One group had greatly reduced k_{pols} values in the presence of Mg^{2+} but responded to Mn^{2+} which restored the k_{pol} values for the nucleotidyl transfer reaction to near wild-type levels. The other group of mutants also had lower k_{pol} values, relative to that of the wild-type polymerase, but could not be rescued by Mn^{2+}. The behavior of these mutants was interpreted in terms of the crystal structures of the available RB69 pol complexes. Our results on the metal ion dependence of the D621A and E686A mutants, together with knowledge of the position of their side chains in two different RB69 pol conformations, suggest that these acidic residues serve as alternative ligands for the metal ions destined to occupy the A and B catalytic sites. We infer that this occurs prior to the conformational change that produces the ternary RB69 pol complex in which the A and B metal ions are ligated by D623 and D411 as the enzyme is poised for phosphoryl transfer.

DNA polymerases play a central role in faithfully transmitting genetic information from parental cells to their progeny. All DNA polymerases catalyze a nucleotidyl transfer reaction (pol activity) in which nucleotide residues are added to the 3′-terminus of a primer strand. Many polymerases have an associated 3′−5′ exonuclease activity either in the same polypeptide with the pol activity or in a different subunit that is a component of the replicase (*1*−*4*). Significant progress has been made during the past decade in understanding the mechanism of both the pol and exo reactions. These advances have come from structural, kinetic, and mutagenesis studies of DNA polymerases from many different sources (for reviews, see refs *5*−*8*). Taken together, the results have provided ample support for a two-metal ion catalytic mechanism for both of these activities, and this mechanism appears to be applicable across all DNA polymerase families (*1*, *9*, *10*).

Members of the B family of DNA polymerases, which includes RB69 DNA polymerase (RB69 pol), are the key components of the replication apparatus. We have focused our efforts on RB69 pol, a T-even phage DNA polymerase, that is remarkably similar in sequence to eukaryotic DNA polymerases and is a good model for studying the detailed mechanisms of both the pol and exo reactions. Its suitability as a prototype B family DNA polymerase is described here. (i) The crystal structures of three different forms of the polymerase have been determined (*11*−*13*). (ii) The minimal kinetic scheme for the closely related T4 DNA polymerase (T4 pol) has been determined (*14*). (iii) The interactions with other proteins that comprise the replicase have been well characterized so that the basic outline of the architecture and function of this multimeric complex can be clarified (*15*, *16*). (iv) The consequences of site specific alterations of conserved residues in RB69 pol can be studied *in vivo* with respect to the type and frequency of mutations produced in the phage genome (*17*). Despite the wealth of information that has been obtained for DNA polymerases, there are still some puzzling issues with regard to structure and function that have not been adequately addressed. Among these is the dynamic relationship between the divalent metal ions in the pol active site and the residues that serve as their ligands in the various conformational states of the enzyme. In the ternary, pol mode complex of RB69 pol, there are two highly conserved residues, D411 and D623, that are essential for catalysis as their carboxylate side chains bind the two catalytic metal ions in the pol active center (*13*). However, there are indications from the crystal structures that other acidic residues may serve as ligands for the catalytic metal ions when the conformational state of the polymerase is altered (*12*). To identify residues other than D411 and D623 that might be involved in nucleotidyl transfer, we constructed several active site RB69 pol mutants having single-site replacements of relatively well conserved residues in the palm and fingers domains. In this paper, we report the properties of these mutants with respect to their ability to function with Mg^{2+} and Mn^{2+}. We have attempted to interpret our results within the framework of the crystal structures of RB69 pol and its complexes with primer−template motifs (P/Ts)[1] and dNTPs. We present a scheme

† This work was supported by United States Public Health Service Grant GM54627-04.

* To whom correspondence should be addressed. Telephone: (203) 785-4599. Fax: (203) 785-7979. E-mail: William.Konigsberg@yale.edu.

[1] Abbreviations: P/T, primer−template; dNTP, deoxynucleoside triphosphate.

10.1021/bi049615p CCC: $27.50
Published on Web 05/07/2004

that contrasts the proposed dynamic nature of metal ion binding in the pol site with the static metal ion binding exhibited by the exo domain.

MATERIALS

Escherichia coli strain BL21(DE3) was obtained from Stratagene Corp. DH5α cells were from Invitrogen. dNTPs, restriction endonucleases, and T4 polynucleotide kinase were purchased from New England Biolabs. [γ-^{32}P]ATP was obtained from Perkin-Elmer Life Sciences Inc. Agarose−Ni−NTA resin was obtained from Qiagen. Other chemicals were analytical grade. The primer (5′-CCGACCACGGAAC) and template (5′-AAAAAACGTTCCGTGGTCGG) were synthesized by the W. M. Keck Foundation Biotechnology Resource Laboratory (Yale University). The plasmid encoding RB69 DNA pol (pCW19) was a gift from J. Karam (Tulane University, New Orleans, LA).

METHODS

Construction of RB69 pol Mutants and Preparation of Proteins. Site-directed mutagenesis was used to introduce Ala for Asp replacements at residues 222 and 327. An exo$^-$ RB69 DNA pol was required so that the K_d and k_{pol} values for mutants having low pol activity could be estimated. Any residual exo activity in the enzyme preparations had to be removed by further purification; otherwise, it would have interfered with the primer extension assays. The RB69 DNA pol mutants reported here were all constructed using the Quikchange procedure (Stratagene) and introduced into the exo$^-$ RB69 DNA pol background. Expression and purification of RB69 DNA pol mutants polymerases were carried out as described previously (*18*); however, we recloned the cDNA for RB69 DNA pol into the pET21 vector (Invitrogen) so that the expressed protein would have six histidine residues appended to its C-terminus.

Chemical-Quench Experiments. All reactions were performed in the KinTek quench-flow instrument (model RQF-3, KinTek Corp., Austin, TX). Burst experiments were performed at 25 °C by mixing 16.5 μL of a solution containing 600 nM enzyme, 2 μM 5′-^{32}P-labeled P/T, 8 mM EDTA in assay buffer [66 mM Tris-HCl (pH 7.5)] with 16.5 μL of 2 mM dGTP, and either 28 mM $MgCl_2$ or 48 mM $MnCl_2$ in assay buffer. Reactions were quenched with 86 μL of 0.5 M EDTA. Single-turnover experiments were carried out at 25 °C by mixing equal volumes (16.5 μL) of assay buffer containing 400 nM 5′-^{32}P-labeled P/T, 8 mM EDTA, and 2 μM enzyme with different concentrations of the complementary dNTP in the same assay buffer that also had either 28 mM $MgCl_2$ or 48 mM $MnCl_2$. The pol reaction was quenched with 0.5 M EDTA at different times. The disappearance of the substrate and the formation of the product were analyzed after they were separated by gel electrophoresis (20% polyacrylamide and 50% urea) and quantified by gel scanning using a phosphorimager (Molecular Dynamics).

Data Analysis. Data obtained from kinetic assays were fitted using Sigma Plot (Jandel Scientific) with the appropriate equations. Data from the chemical-quench experiments were fit to a single-exponential equation. Data for the dependency of k_{obs} as a function of dNTP concentration were fit to the equation $k_{obs} = k_{pol}[dNTP]/(K_d + [dNTP])$, where k_{obs} is the observed first-order rate constant, k_{pol} is the rate of dNMP incorporation, K_d is the equilibrium dissociation constant for dNTP, and [dNTP] is the concentration of deoxynucleoside triphosphate.

RESULTS AND DISCUSSION

Our principal goal in this study was to realize a better understanding of how certain conserved residues in the palm domain affected the pol reaction, particularly with respect to divalent metal ions. From previous reports on human pol α and ϕ29 pol, members of the B family of DNA polymerases, we knew that replacement of many of the conserved residues in the palm domain led to reductions in the steady-state k_{cat} values, in some cases by more than 100-fold relative to the value for wild-type DNA polymerase (*19*−*21*). While these studies have identified residues involved in binding and catalysis, they have not provided deeper insights into the mechanistic details of the nucleotidyl transfer reaction because steady-state parameters include steps after chemistry such as product dissociation or P/T translocation which are often rate-limiting. Since neither crystal structures nor pre-steady-state kinetic parameters were available for these two B family DNA polymerases, only limited structure−function correlations could be made, and these were based on minimal sequence similarities with the Klenow fragment (*22*, *23*). We therefore decided to limit our study to RB69 pol, since crystal structures of three different complexes of this polymerase have been determined (*11*−*13*). The structures of these complexes guided us in selecting residues for replacement and gave us a framework for interpreting pre-steady-state kinetic results obtained with single-site mutants. We chose rapid, chemical-quench techniques for obtaining data that would provide more information about the role of the conserved residues in the various steps required for primer extension. In particular, we were interested in the possibility that some of the residues selected for replacement were involved in the metal ion-dependent phosphoryl transfer reaction. The following residues were targeted: D621, T622, S624, Y619, E686, E716, K706, and Y708 (all located in the palm and finger domains as shown in Figures 1 and 2). They were replaced with Ala, except for S624 which was replaced with Cys, Y619 with Phe, and K706 with Arg.

Results from single-turnover experiments showed that the mutants could be divided into two groups. Mutants in the first group all had greatly reduced k_{pol} values with Mg^{2+}; however, their activity increased dramatically in the presence of Mn^{2+} ions (Table 1). Mutants in the second group also had lower k_{obs} values, but their activity could not be rescued by Mn^{2+} (Table 2).

Kinetic Behavior of Group 1 Mutants whose Activity Was Restored by Manganese Ions. Two highly conserved residues, D621 and E686, were of special interest because steady-state kinetic results performed earlier in our lab had already shown that the D621A and E686A mutants had much lower activity in the presence of Mg^{2+} (data not shown). In our experiments, we used the same conditions for obtaining pre-steady-state kinetic parameters like those reported by Capson *et al.* in their studies on the mechanism of T4 pol (*14*). We observed k_{pol} and K_d values for the incorporation of dNMPs by the exo$^-$ RB69 pol (parental enzyme) that were close to those observed by Capson *et al.* (*14*) for T4 pol in single-

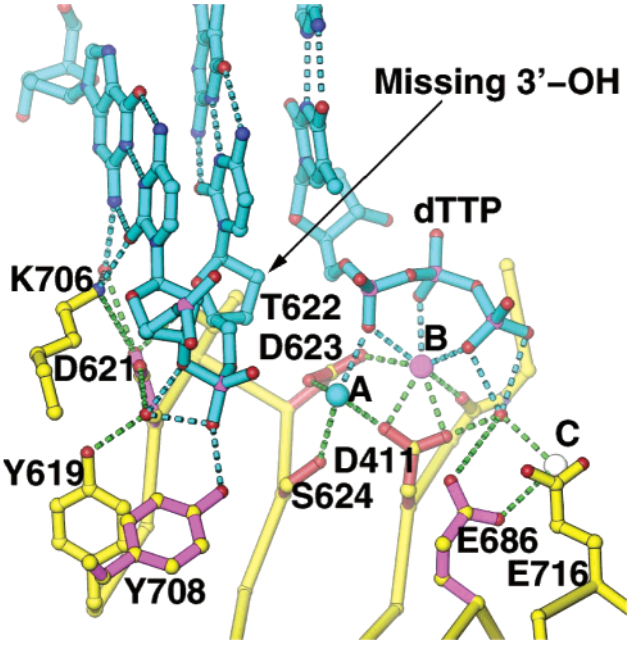

FIGURE 1: Active site in the RB69 DNA polymerase ternary complex with a dideoxy-terminated DNA duplex and dTTP. Residues D411, D623, and S624, which are ligands for the catalytic metal ions (A and B), are shown in red, and ligands which are proposed to be involved indirectly in metal ion binding (D621, E686, and Y708) as revealed in this study (see Table 1) are shown in purple. A noncatalytic metal ion (C) and a water molecule mediate interactions between E686 and the γ-phosphate of dTTP. The P/T and incoming dTTP are shown in blue. The dashed lines represent hydrogen bonds and metal ion−ligand interactions. The figure is based on the structural work of Franklin *et al*. (*13*).

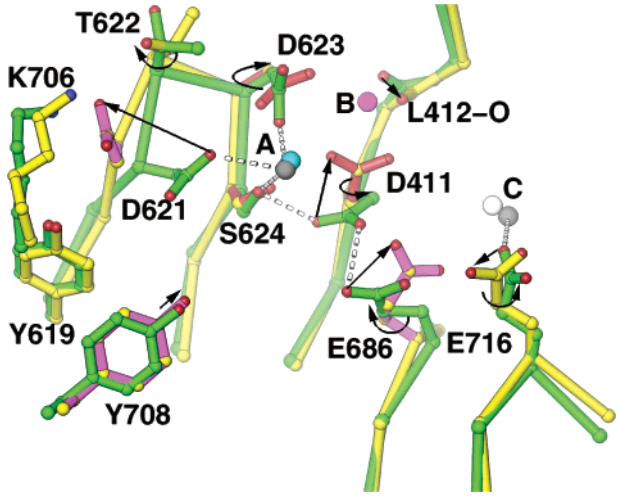

FIGURE 2: Comparison of the pol active site between the binary complex (green) (*12*) and the ternary complex (yellow) (*13*). Only two metal ions, A and C (gray), are present in the binary complex and are coordinated by D621, D623, S624 (metal ion A), and E716 (metal ion C). Large conformational changes occur in the side chains of D411, D621, T622, D623, E686, and E716 and the carbonyl group of the L412 peptide bond.

turnover experiments (Table 1). In addition, we found that the optimal Mg^{2+} and Mn^{2+} concentrations for both RB69 pol and the mutants reported here were 10 and 20 mM, respectively. To determine active site concentrations and whether steps after chemistry were rate-limiting, we carried out burst experiments with excess P/T over enzyme and with saturating dNTP concentrations. We found that the E686A and D621A mutants had nearly identical amplitudes (~300)

Table 1: Single-Turnover Kinetic Parameters[a] for the Parental RB69 Pol and Its Mutants with either Mg^{2+} or Mn^{2+}

	Mg^{2+}		Mn^{2+}	
RB69 pol	k_{pol} (s^{-1})	K_d with dGTP (μM)	k_{pol} (s^{-1})	K_d with dGTP (μM)
parental exo$^-$	170 ± 10	25 ± 5	200 ± 15	20 ± 4
D621A	1.3 ± 0.1	166 ± 40	112 ± 8	34 ± 6
E686A	7 ± 0.2	58 ± 7	200 ± 29	13 ± 3
S624C	4.5 ± 0.5	18 ± 3	108 ± 11	20 ± 4
Y708A	6 ± 0.4	34 ± 7	74 ± 3	14 ± 3

[a] Conditions: 1000 nM enzyme, 200 nM P/T, different concentrations of dGTP, 10 mM $MgCl_2$ or 20 mM $MnCl_2$, 66 mM Tris-HCl, pH 7.5, and 25 °C. Number of experiments performed: five for the parental enzyme, three for D621A and E686A, and two for S624C and Y708A.

Table 2: Rates of Incorporation of dGTP under Single-Turnover Conditions[a] for RB69 Pol Mutants with Mg^{2+} and Mn^{2+}

	k_{obs}[b] (s^{-1})	
RB69 pol mutant	Mg^{2+}	Mn^{2+}
Y619F	14 ± 1	21 ± 1
K706A	0.1 ± 0.01	0.2 ± 0.02
K706R	20 ± 2	31 ± 4
T622A	0.2 ± 0.02	0.2 ± 0.04
E716A	200 ± 40	200 ± 28

[a] Conditions: 1000 nM enzyme, 200 nM P/T, 1 mM dGTP, 10 mM $MgCl_2$ or 20 mM $MnCl_2$, 66 mM Tris-HCl, pH 7.5, and 25 °C. Number of experiments performed: three for Y619F and two for K706A, K706R, T622A, and E716A. [b] k_{obs} is the rate of incorporation of dGMP at a dGTP concentration of 1 mM. This is ~50 times the K_d for the parental enzyme and is likely to be saturating for these four mutants and therefore would approximate k_{pol}.

which were close to the concentration of the enzymes in the reaction mixtures when Mg^{2+} or Mn^{2+} was present (Figure 3). The burst experiments for E686A and D621A fit best to burst equation $y = A[1 - \exp(-k_1 t)] + rt$, where y is the concentration of the product, A is the amplitude, k_1 is the observed "burst" rate constant, and r is the observed linear rate. We estimated k_{cat} from the second phase of the exponential by dividing r by the amplitude. For the D621A mutant, k_{cat} equaled 0.02 s^{-1} with Mg^{2+} but increased to 0.08 s^{-1} with Mn^{2+}. For the E686A mutant, k_{cat} equaled 0.04 s^{-1} with both Mg^{2+} and Mn^{2+}. The results obtained for single-turnover experiments with the parental enzyme and the D621A mutant using Mg^{2+} and Mn^{2+} at saturating dGTP concentrations are shown in Figure 4A−D. An example of the data used in estimating the k_{pol} and K_d for the E686A and D621A mutants with dGTP and Mg^{2+} and Mn^{2+} is shown in Figure 5. The same conditions for the single-turnover experiments were used with all of the mutants. For the E686A mutant, the k_{pol} values in the presence of Mg^{2+} were reduced dramatically, but Mn^{2+} restored the activity to wild-type levels. The pre-steady-state kinetic behavior of the D621A mutant in the presence of either Mg^{2+} or Mn^{2+} under single-turnover conditions (Table 1) was consistent with the steady-state results reported for the corresponding D456G mutant of ϕ29 pol, another member of the B family of polymerases (*21*).

Although the conservation and involvement of the three acidic residues, D411, D623, and D621 [which are part of motifs A and C (*11*, *22*)], in the pol reaction have been reported for many other polymerases, no mutants corresponding to RB69 pol E686A in any of the B family DNA

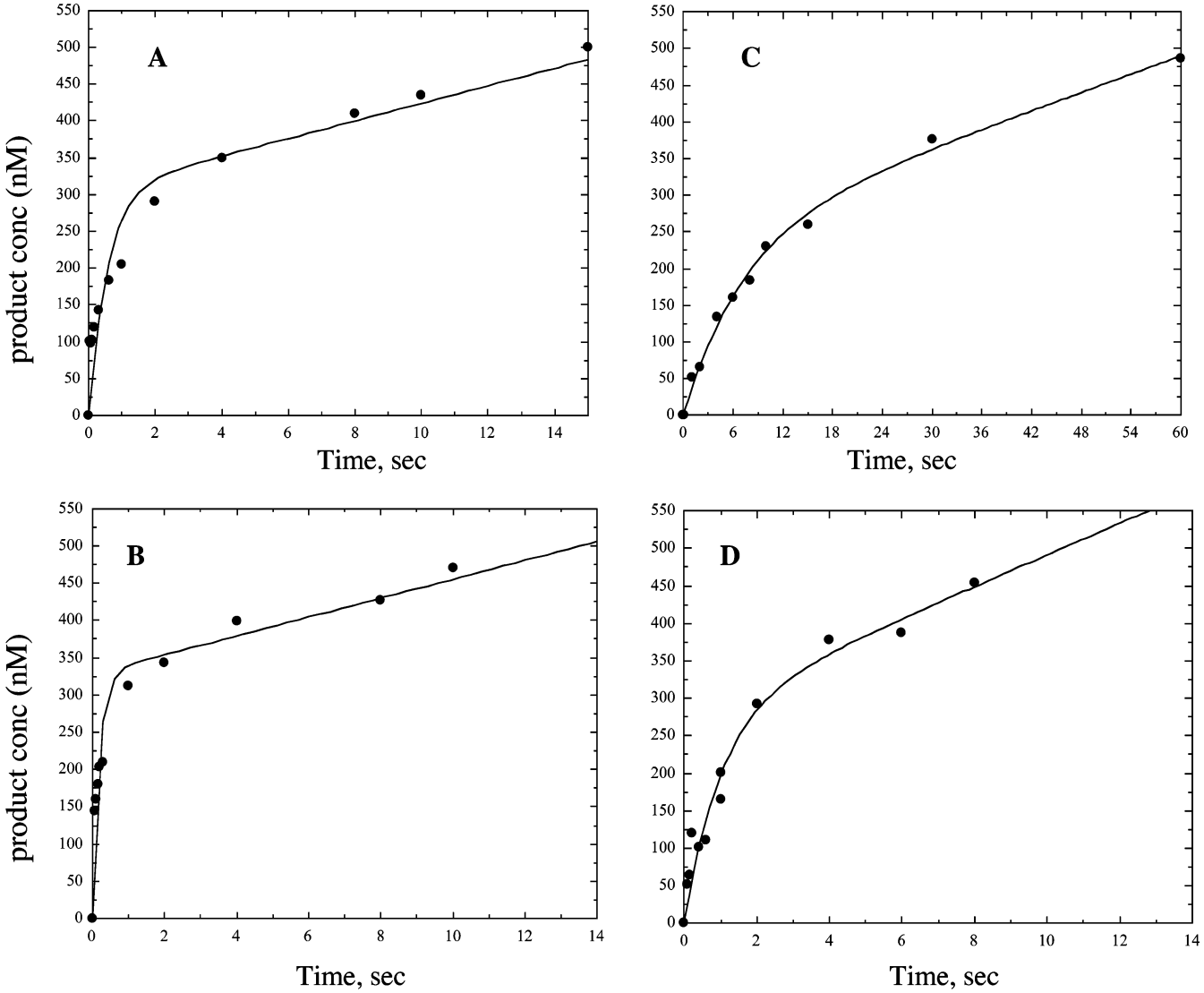

FIGURE 3: Rapid-quench experiments were carried out by mixing 16.5 μL of 600 nM enzyme and 2 μM 5′-^{32}P-labeled P/T in assay buffer (pH 7.5) in syringe A with 16.5 μL of 2 mM dGTP and either 20 mM $MgCl_2$ or 40 mM $MnCl_2$ in syringe B. Reactions were quenched with 86 μL of 0.5 M EDTA. (A) E686A with 10 mM $MgCl_2$: $A = 304$, $k_1 = 1.8$ s^{-1}, and $r = 12$ nM/s^{-1}. (B) E686A with 20 mM $MnCl_2$: $A = 320$, $k_1 = 5.2$ s^{-1}, and $r = 13$ nM/s^{-1}. (C) D621A with 10 mM $MgCl_2$: $A = 242$, $k_1 = 0.14$ s^{-1}, and $r = 4.1$ nM/s^{-1}. (D) D621A with 20 mM $MnCl_2$: $A = 279$, $k_1 = 1$ s^{-1}, and $r = 21.2$ nM/s^{-1}. The products were analyzed and quantified as described in Methods. The data were fit to the burst equation using Sigma Plot.

pols have been described. The aforementioned results were puzzling in view of the fact that there is no indication from the crystal structure of the RB69 pol ternary complex that D621 or E686 interacts directly with the P/T, the incoming dNTP, or either of the two catalytic metal ions (*13*). However, our kinetic data with Mn^{2+} suggest that these residues are indirectly involved in metal ion coordination. As discussed below, this suggestion can be rationalized on the basis of structures determined for other RB69 pol complexes and by analogy with structural information from different DNA polymerases. Experiments with mutants whose activity could not be restored by Mn^{2+} are also consistent with the indirect involvement of D621 and E686 in ligating the catalytic metal ions. For example, Mn^{2+} cannot restore even minimal activity to the D411A and D623A mutants (data not shown), a result that was expected since both D411 and D623 are directly involved in metal ion binding in the catalytically active ternary complex. Also, as shown below, residues that have no involvement with metal ions, when mutated, cannot be rescued by Mn^{2+}.

Are Alternative Metal Ion Ligands Used in the Reaction Cycle? In contrast to the exo domain, where two metal ion binding sites are largely defined by conserved carboxylates and remain fixed during all steps of nucleotide excision (*12*), the situation with respect to the pol active site is more dynamic. In the exo reaction, the single-stranded DNA substrate enters the exo site without bound metal ions, and the product, a nucleoside monophosphate, leaves the exo site without an accompanying metal ion. In the pol active center, we propose that the metal ion binding sites shift during the polymerization cycle based on the following observations. In the ternary complex, three metal ions were observed. Catalytic metal ions A and B are coordinated with D411 and D623, and metal ion C appears to be ligated by E716 and was one of the residues we selected for replacement (*13*). The triphosphate tail of the incoming dNTP also coordinates

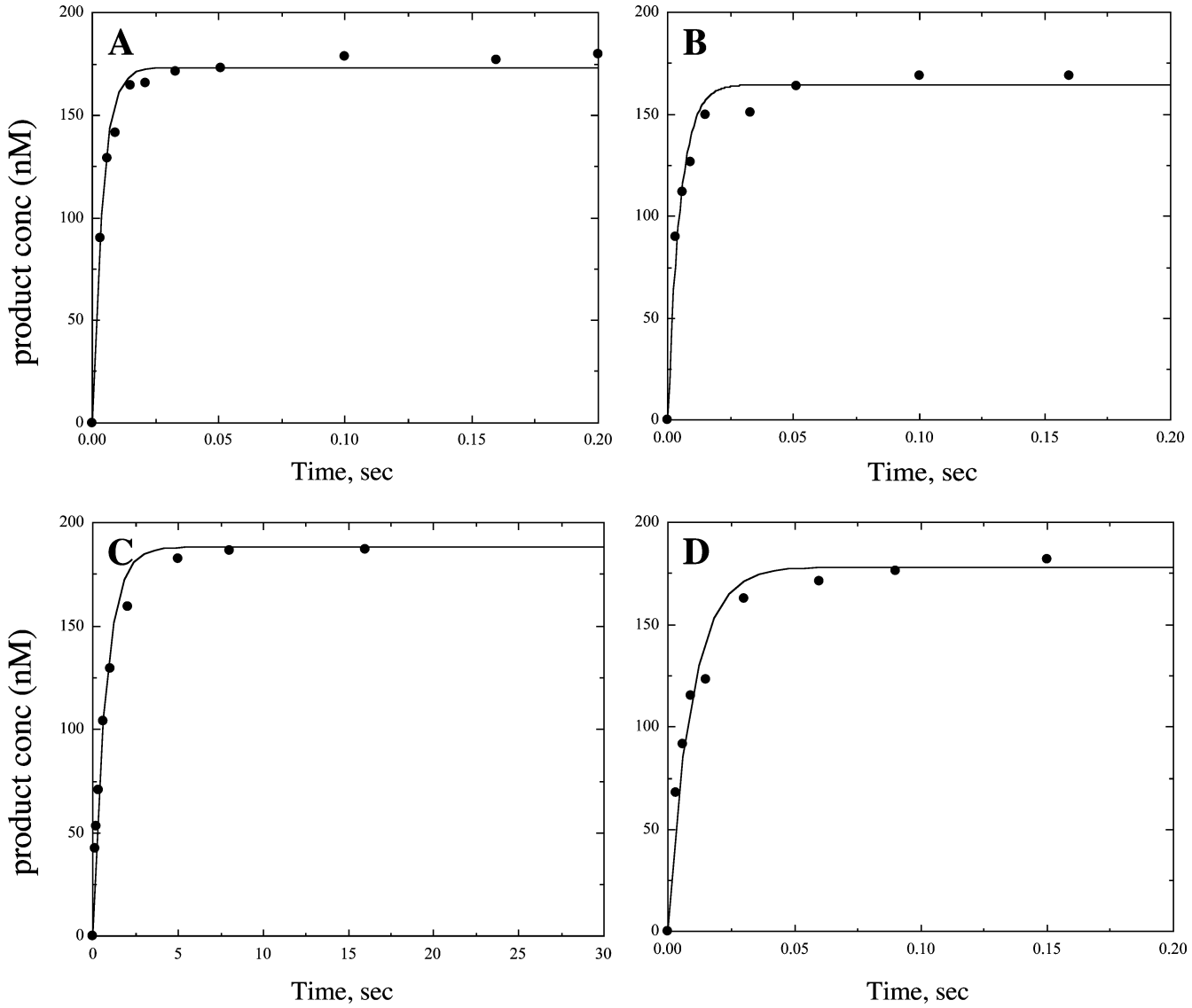

FIGURE 4: Determination of the rate of dGMP incorporation into 13/20mer P/T using the parental RB69 pol and the D621A mutant. Reactions were carried out under single-turnover conditions by mixing 16.5 μL of 2 μM enzyme and 400 nM 5′-^{32}P-labeled P/T in assay buffer (pH 7.5) with 16.5 μL of 1 mM dGTP and either Mg^{2+} or Mn^{2+} in the same reaction buffer: (A) parental enzyme with 10 mM $MgCl_2$, (B) parental enzyme with 20 mM $MnCl_2$, (C) D621A with 10 mM $MgCl_2$, and (D) D621A with 20 mM $MnCl_2$. The data were fit to a single-exponential equation using Sigma Plot.

both the A and B metal ions. In the binary enzyme−P/T complex, only two metal ions, A and C, are observed but in slightly different positions compared to their locations in the ternary complex (Figure 2). No B metal ion is seen in the binary complex because the B site is not fully formed prior to the entry of the dNTP.

After binding of the complementary dNTP, the enzyme−P/T complex undergoes a conformational change to form a catalytically competent ternary complex. *In vivo*, the incoming dNTP is coordinated with Mg^{2+}, but when it binds to an enzyme−P/T complex, a B site is generated by swiveling of the D411 and D623 side chains so that their carboxylates point toward the incoming B metal ion, thus forming a nearly optimal octahedral coordination complex that includes the peptide backbone carbonyl oxygen of L412 (Figures 1 and 2). This high-affinity site binds the B metal ion until the chemical step is completed. Following chemistry, the protein undergoes another conformational change that disrupts the B site and facilitates dissociation of pyrophosphate that leaves together with the B metal ion. Translocation can now occur so that the P/T becomes properly positioned for binding and incorporation of the next dNMP. As a consequence of this conformational change, the side chains of D411 and D623 rotate again so that the carboxylates no longer point toward each other, thus relieving electrostatic repulsion of their negative charges. In addition, the carbonyl oxygen of the L412 peptide bond, one of the ligands for metal ion B in the ternary complex, shifts its position. As can be seen in Figure 2, D623 is still close to metal ion A but D411 is not, making it unlikely that D411 is a ligand for metal ion A at this point in the reaction cycle.

The binary enzyme−P/T structure also has other acidic residues that are in a position to coordinate a metal ion in an uncharacterized location which is close to the position that metal ion A would occupy in the ternary complex. In addition to D623 and D411, three highly conserved residues, D621, E686, and E716, are near the active site. The side chains of these residues are reoriented when the enzyme

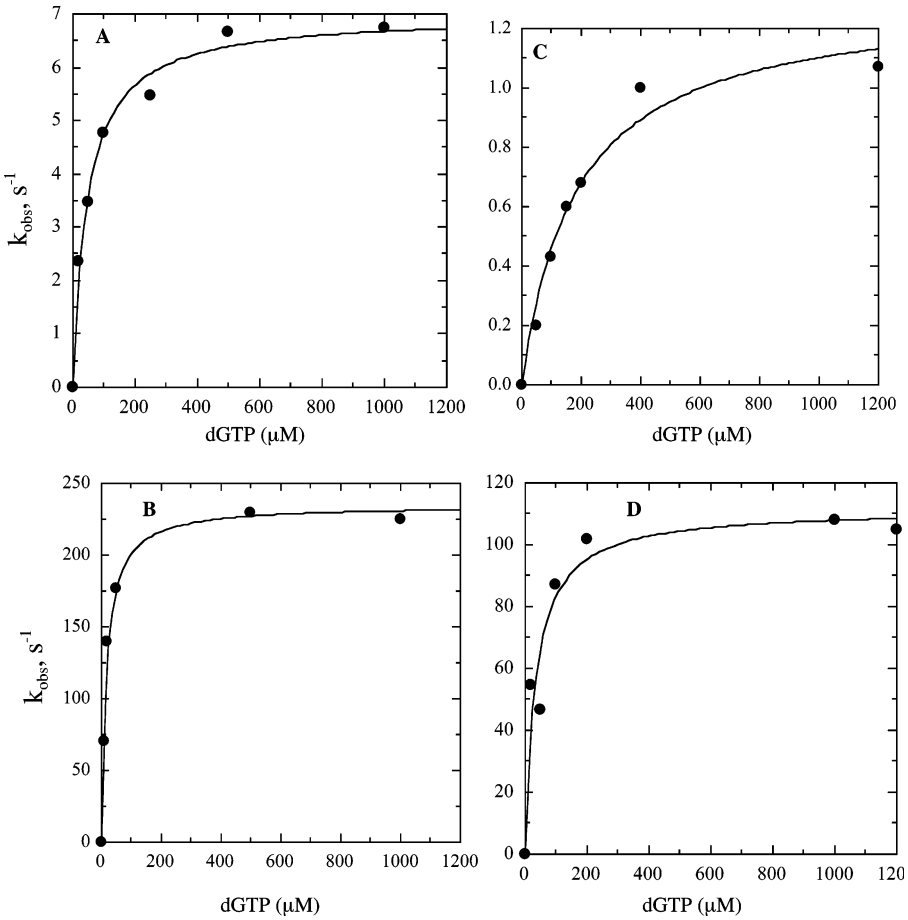

FIGURE 5: Determination of K_d (dGTP) for the RB69 pol E686A and D621A mutants with Mg^{2+} and Mn^{2+}. Reactions were carried out under single-turnover conditions by mixing 16.5 μL of 2 μM enzyme and 400 nM 5′-^{32}P-labeled P/T in assay buffer (pH 7.5) with 16.5 μL of dGTP at varying concentrations and either Mg^{2+} or Mn^{2+} in the same assay buffer in syringe B. Reactions were carried out at 25 °C and quenched with 86 μL of 0.5 M EDTA. The products were analyzed and quantified as described in Methods: (A) k_{obs} vs [dGTP] with 10 mM $MgCl_2$ for E686A, (B) k_{obs} vs [dGTP] with 20 mM $MnCl_2$ for E686A, (C) k_{obs} vs [dGTP] with 10 mM $MgCl_2$ for D621A, and (D) k_{obs} vs [dGTP] with 20 mM $MnCl_2$ for D621A. The data were fit to the hyperbolic equation (see Methods) using Sigma Plot.

switches from the ternary to the binary complex after the addition of a nucleotide residue during primer extension.

Relative Positions of D621 and E686 in the Different RB69 pol Complexes. As mentioned above, metal ion A is ligated by D411 and D623 in the ternary complex as shown in Figure 1, but in the binary complex, the A metal ion shifts by 0.5 Å and is coordinated by D623 and D621 instead of D411, which now points away from the active site. In the ternary complex, D621 interacts with O2 of the second base pair of the P/T duplex in the minor groove via a hydrogen bond to another conserved residue, K706 (Figure 1). Structural alignment fails to show a residue equivalent to D621 in the pol I family of DNA polymerases such as KF and Taq (*11*), suggesting that D621, which is highly conserved in the B family, might have an indirect functional role in the phosphoryl transfer reaction with enzymes in this group. This view is supported by pre-steady-state kinetic results which show that the k_{pol} for the D62A mutant was reduced by 116-fold; however, its activity could be restored by Mn^{2+} to ~60% of the wild-type level (Table 1). The conserved residue, E686, appears to be a considerable distance from the metal ion binding sites in the ternary complex but is within 2.5 Å of the third metal ion (metal ion C, Figure 1) (*13*). The E686A mutant has a lower k_{pol} than the parental enzyme, but its activity can also be restored to wild-type levels by Mn^{2+} (Table 1).

The kinetic results support a dynamic functional role for D621 and E686 that is not evident from the structure of the ternary complex. We propose that these residues are involved in controlling the divalent ion movement during the polymerization cycle. They may also help to position the primer terminus and the triphosphate tail of the incoming dNTP. We suggest that D621 is a transient ligand for metal ion A since, in the binary complex, D621 is in a position to interact with metal ion A (Figure 2). During assembly of the ternary complex, metal ion A can be transferred from D621 to its final position where it is ligated by D623 and D411 in the active site. In going from the binary to the ternary complex, D621 must release metal ion A; otherwise, its continued coordination by D621 would interfere with its ligation by D411 and D623. After chemistry, metal ion A is probably released from the active site, where it can either be religated by D621 or diffuse into the solvent. If the latter situation occurs, then D621 would have to capture another divalent metal ion to continue the polymerization cycle. Clearly, the effect of Mn^{2+} on the E686A mutant suggests that E686 also has a metal ion-dependent role in the pol reaction, but it is not obvious which metal ion or at what stage of the reaction cycle it is involved. E686 might have a role in coordinating metal ion B which is also ligated by the triphosphate tail of the incoming dNTP and probably has a role in positioning the dNTP, as implied from the 22-fold reduction in k_{pol}

observed with the E686A mutant. The formation of the catalytically competent complex requires the fingers domain to rotate 60° toward the palm, locking the dNTP in the active site (*13*). Accompanying this rotation is a reorientation of E686, located in the palm domain, which allows its carboxyl group to bind metal ion C. This metal ion interacts indirectly with the γ-phosphate of dNTP through an ordered water molecule (the only other interaction that is observed with this metal ion) (Figures 1 and 2). This interaction may also help to properly position the dNTP for nucleophilic attack by the 3′-hydroxyl group of the primer.

Possible Function of Other Metal-Dependent Group 1 Mutants. Four of the group 1 mutants had reduced k_{pol} values (from 25- to 130-fold), but regained partial or full activity with Mn^{2+}. We interpret this as an indication that these residues are involved in the formation and disruption of metal ion binding sites. There is only a single residue, S624, that serves as a common ligand for metal ion A as it shuttles between binary and ternary complexes during polymerization. As predicted, the S624C mutant has a lower k_{pol} (Table 1). From the observed rotomer conformation of the S624 side chain, it is likely that there is a hydrogen bond between the hydroxyl group of S624 and the carboxylate oxygen of D411 (*13*) which stabilizes the position of the D411 carboxylate so that it has the optimal geometry for binding metal ion A (Figures 1 and 2). Substitution of Cys for Ser624 would be expected, from modeling, to cause a steric clash between the Cys sulfur atom and one of the carboxyl oxygens of D411. To relieve this, the side chain of D411 must assume a different rotomer conformation, perturbing its interaction with metal ion A, and this, in turn, could account for the lower k_{pol} of the S624C mutant.

The low activity of the Y708A mutant and its partial rescue by Mn^{2+} (Table 1) can be rationalized as follows. Replacement of Y708 with Ala eliminates the hydrogen bond between the γ-OH group of Y708 and the nonbridging oxygen of the 3′-terminal phosphodiester bond in the primer (Figure 1). This would be expected to destabilize the conformation of the 3′-terminal nucleotide residue and consequently reduce k_{pol} in the presence of Mg^{2+}. When Mn^{2+} rather than Mg^{2+} ions are used, the Mn^{2+} may actually reduce the conformational flexibility of the 3′-terminus via hydrogen bonding of a Mn^{2+}-ligated water molecule to the nonbridging oxygen in the terminal phosphodiester linkage.

Why is Mn^{2+} able to increase the pol activity of group 1 mutants? Although it is well-known that Mn^{2+} affects pol activity, the principal effect is the ability of Mn^{2+} to reduce base selectivity, resulting in an increased frequency of misincorporation (*19*, *20*, *24*−*28*). With T4 pol, Mn^{2+} appears to strengthen the binding of mispaired nucleotides to the P/T (*29*). With pol β, the level of base discrimination is also reduced in the presence of Mn^{2+}. This has been ascribed to tighter nucleotide binding and to the higher reactivity of Mn^{2+} which undergoes ligand exchange more readily (by a factor of 100) than Mg^{2+} (*30*, *31*). These properties exhibited by Mn^{2+} might also be relevant to the rescue of the pol activity of group 1 mutants by Mn^{2+}. In addition to these properties, the following differences between Mg^{2+} and Mn^{2+} may also contribute to the ability of the RB69 pol group 1 mutants to efficiently catalyze nucleotidyl transfer in the presence of Mn^{2+}: (i) the larger radius of Mn^{2+} compared to Mg^{2+} (0.86 Å vs 0.60 Å) (*32*), (ii) the presence of d orbital electrons in the Mn^{2+} outer shell, and (iii) the observation that Mn^{2+} binds to the triphosphate tail of dNTP as in an α,γ bidentate complex in contrast to Mg^{2+} which binds to dNTPs in a β,γ bidentate complex (*33*). Clearly, crystal structures of some of the mutants, such as D621A or E686A with Mn^{2+} in a ternary complex, would help to explain the Mn^{2+} rescue phenomenon. Also, crystal structures of RB69 pol complexes trapped in conformations other than the three already reported would help to provide more direct evidence for the role of these proposed alternative metal ion ligands in the reaction cycle.

Kinetic Behavior of Group 2 Mutants whose Activity Could Not Be Restored by Mn^{2+}. To show that Mn^{2+} rescue was not an intrinsic property exhibited by this metal ion, we picked other mutants with reduced pol activity as controls. We determined the k_{obs} values for these mutants under single-turnover conditions with saturating amounts of dGTP. Among the mutants whose pol activity could not be rescued by Mn^{2+}, T622A and K706A exhibited the largest decrease in k_{obs} relative to that of the parental enzyme. In the ternary structure, the OH group of T622 is hydrogen-bonded to an internal network of water molecules that help position the side chains of T587 and Y416 (the "sugar gate" residue) as well as the backbone amide nitrogen of F395 (see Figure 2B in ref *34*). If the OH group of T622 is absent, the hydrogen bonding network is compromised and the position of the side chain of Y416 would not remain fixed. This might interfere with the orientation of the sugar residue of the incoming dNTP, resulting in the greatly diminished k_{obs} found when T622 was changed to Ala. This hydrogen-bonded network of water molecules is far from the metal ion sites so it was not surprising that Mn^{2+} failed to increase the pol activity of this mutant. The fact that the K706A mutant has a 1000-fold reduction in k_{pol} and cannot be rescued by Mn^{2+} is consistent with the ternary structure where the ϵ-amino group of K706 links the D621 carboxylate to O2 of the penultimate base at the 3′-end of the primer (Figure 1). It would appear that the electrostatic interaction between K706 and D621 competes effectively with the ability of D621 to serve as a ligand for the A metal ion. The K706A mutant obviously cannot help to reorient the D621 carboxyl group, but the K706R mutant can by virtue of its positive charge, although not as effectively as K706 itself. This is borne out by the 10-fold reduction in k_{obs} for K706R rather than the 1000-fold drop found for the K706A mutant (Table 2). The failure of Mn^{2+} to affect k_{obs} with either the K706A or the K706R mutant was expected, given the large distance between the side chain of either the K706A or K706R mutant and the A metal ion site.

Residue Y619 also participates in a hydrogen bonding network via a water molecule situated between the Tyr hydroxyl group and the nonbridging oxygen in the terminal phosphodiester linkage of the primer (Figure 1) (*13*). In the absence of these hydrogen bonds, the residence time of the 3′-terminal deoxyribosyl moiety in the pol active site might be expected to decrease and so would the k_{obs} for the Y619F mutant. As observed with the K706R mutant, k_{obs} is reduced by ~15-fold for the Y619F mutant relative to the parental enzyme, and again, because of its distance from metal ion A, we anticipated that the activity would not be rescued by Mn^{2+}. This expectation was realized (Table 2), but it should be noted that, in contrast to our results, steady-state kinetic

assays with human pol α mutants T1003N and Y1000F (corresponding to T622A and Y619F, respectively, in RB69 pol) showed an increase in pol activity when Mn^{2+} was substituted for Mg^{2+} (*20*).

Finally, E716 appears to interact with metal ion C in the editing complex (*12*) but not in the ternary complex (*13*). Its replacement with Ala has no effect on catalysis (Table 2); thus, the functional significance of E716 remains in doubt.

Evidence from Other DNA Polymerases for Dynamic Metal Ion Binding Sites. The notion that residues other than those observed in the ternary RB69 pol complex could be involved in coordinating the divalent metal ions has been suggested for other polymerases. For example, with HIV-RT, Sarafianos *et al*. (*35*) proposed that, while the B metal ion is released with PP_i after the nucleotidyl transfer reaction, the A metal ion moves in and out of the position required for catalyzing the phosphoryl transfer. This displacement is accompanied by torsional movements of D185 and D186. In one conformation, the carboxylate oxygen of D186 is 2.3 Å from the A metal ion, but in the ternary complex, it is too distant to serve as a ligand (*35*). This scenario is reminiscent of the one we have proposed for D621 in RB69 pol. With T7 DNA pol, computer simulations (*36*, *37*), compared with structural data (*38*), indicate that different Asp residues can act as ligands for metal ion A at different times during the cycle of dNTP binding, transfer, and P/T translocation. For the Klenow fragment, Gangurde *et al*. (*39*) have proposed that either E710 or E883 is required for the pol reaction in the active carboxylate triad (D705, D882, and E710 or E883) (*39*). Their results suggest that E710 or E883 might act as an alternative ligand for metal ion A in a precatalytic ternary complex or that a critical hydrogen bonding interaction is disrupted when either of the Glu residues is replaced. An analogous situation has been described with pol β, where there appears to be rotation of the Asp256 side chain, one of the three highly conserved active site carboxylate-containing residues that facilitates metal ion A binding during catalysis (*40*, *41*). It has also been reported that the torsion angle of the D192 side chain bends it away from the active site, enabling it to form a strong hydrogen bond with R258. Once metal ions bind in the catalytic metal ion sites, the torsional angle of D192 is altered, breaking the hydrogen bond with R258 and reorienting the D192 side chain so that it is in a favorable geometry for binding both catalytic metal ions (*32*, *42*). It seems therefore that structurally and evolutionarily diverse DNA polymerases may use similar strategies for catalytic metal ion binding and release. However, no extensive Mn^{2+} rescue experiments have been carried out with other DNA polymerase mutants using the type of strategy reported in this study.

ACKNOWLEDGMENT

We thank Jim Karam (Tulane University) for the RB69 pol cDNA and Liz Vellali for skillful preparation of the manuscript.

REFERENCES

1. Joyce, C. M., and Steitz, T. A. (1994) Function and structure relationships in DNA polymerases, *Annu. Rev. Biochem. 63*, 777−822.
2. Bebenek, K., and Kunkel, T. A. (2002) Family growth: the eukaryotic DNA polymerase revolution, *Cell. Mol. Life Sci. 59*, 54−57.
3. Kunkel, T. A., and Bebenek, K. (2000) DNA replication fidelity, *Annu. Rev. Biochem. 69*, 497−529.
4. Beard, W. A., and Wilson, S. H. (2003) Structural insights into the origins of DNA polymerase fidelity, *Structure 11*, 489−496.
5. Steitz, T. A. (1999) DNA polymerases: structural diversity and common mechanisms, *J. Biol. Chem. 274*, 17395−17398.
6. Doublie, S., Sawaya, M. R., and Ellenberger, T. (1999) An open and closed case for all polymerases, *Struct. Folding Des. 7*, R31−R35.
7. Jager, J., and Pata, J. D. (1999) Getting a grip: polymerases and their substrate complexes, *Curr. Opin. Struct. Biol. 9*, 21−28.
8. Hubscher, U., Maga, G., and Spadari, S. (2002) Eukaryotic DNA polymerases, *Annu. Rev. Biochem. 71*, 133−163.
9. Brautigam, C. A., and Steitz, T. A. (1998) Structural and functional insights provided by crystal structures of DNA polymerases and their substrate complexes, *Curr. Opin. Struct. Biol. 8*, 54−63.
10. Steitz, T. A. (1998) A mechanism for all polymerases, *Nature 391*, 231−232.
11. Wang, J., Sattar, A. K., Wang, C. C., Karam, J. D., Konigsberg, W. H., and Steitz, T. A. (1997) Crystal structure of a pol alpha family replication DNA polymerase from bacteriophage RB69, *Cell 89*, 1087−1099.
12. Shamoo, Y., and Steitz, T. A. (1999) Building a replisome from interacting pieces: sliding clamp complexed to a peptide from DNA polymerase and a polymerase editing complex, *Cell 99*, 155−166.
13. Franklin, M. C., Wang, J., and Steitz, T. A. (2001) Structure of the replicating complex of a pol alpha family DNA polymerase, *Cell 105*, 657−667.
14. Capson, T. L., Peliska, J. A., Kaboord, B. F., Frey, M. W., Lively, C., Dahlberg, M., and Benkovic, S. J. (1992) Kinetic characterization of the polymerase and exonuclease activities of the gene 43 protein of bacteriophage T4, *Biochemistry 31*, 10984−10994.
15. Benkovic, S. J., Valentine, A. M., and Salinas, F. (2001) Replisome-mediated DNA replication, *Annu. Rev. Biochem. 70*, 181−208.
16. Trakselis, M. A., Mayer, M. U., Ishmael, F. T., Roccasecca, R. M., and Benkovic, S. J. (2001) Dynamic protein interactions in the bacteriophage T4 replisome, *Trends Biochem. Sci. 26*, 566−572.
17. Bebenek, A., Dressman, H. K., Carver, G. T., Ng, S., Petrov, V., Yang, G., Konigsberg, W. H., Karam, J. D., and Drake, J. W. (2001) Interacting fidelity defects in the replicative DNA polymerase of bacteriophage RB69, *J. Biol. Chem. 276*, 10387−10397.
18. Yang, G., Lin, T., Karam, J., and Konigsberg, W. H. (1999) Steady-state kinetic characterization of RB69 DNA polymerase mutants that affect dNTP incorporation, *Biochemistry 38*, 8094−8101.
19. Copeland, W. C., Lam, N. K., and Wang, T. S. (1993) Fidelity studies of the human DNA polymerase alpha. The most conserved region among alpha-like DNA polymerases is responsible for metal-induced infidelity in DNA synthesis, *J. Biol. Chem. 268*, 11041−11049.
20. Copeland, W. C., and Wang, T. S. (1993) Mutational analysis of the human DNA polymerase alpha. The most conserved region in alpha-like DNA polymerases is involved in metal-specific catalysis, *J. Biol. Chem. 268*, 11028−11040.
21. Saturno, J., Lazaro, J. M., Blanco, L., and Salas, M. (1998) Role of the first aspartate residue of the "YxDTDS" motif of ϕ29 DNA polymerase as a metal ligand during both TP-primed and DNA-primed DNA synthesis, *J. Mol. Biol. 283*, 633−642.
22. Delarue, M., Poch, O., Tordo, N., Moras, D., and Argos, P. (1990) An attempt to unify the structure of polymerases, *Protein Eng. 3*, 461−467.
23. Braithwaite, D. K., and Ito, J. (1993) Compilation, alignment, and phylogenetic relationships of DNA polymerases, *Nucleic Acids Res. 21*, 787−802.
24. Dong, Q., Copeland, W. C., and Wang, T. S. (1993) Mutational studies of human DNA polymerase alpha. Serine 867 in the second most conserved region among alpha-like DNA polymerases is involved in primer binding and mispair primer extension, *J. Biol. Chem. 268*, 24175−24182.
25. Dong, Q., Copeland, W. C., and Wang, T. S. (1993) Mutational studies of human DNA polymerase alpha. Identification of residues critical for deoxynucleotide binding and misinsertion fidelity of DNA synthesis, *J. Biol. Chem. 268*, 24163−24174.
26. Tabor, S., and Richardson, C. C. (1989) Effect of manganese ions on the incorporation of dideoxynucleotides by bacteriophage T7 DNA polymerase and *Escherichia coli* DNA polymerase I, *Proc. Natl. Acad. Sci. U.S.A. 86*, 4076−4080.

27. Blanco, L., Prieto, I., Gutierrez, J., Bernad, A., Lazaro, J. M., Hermoso, J. M., and Salas, M. (1987) Effect of NH^{4+} ions on ϕ29 DNA-protein p3 replication: formation of a complex between the terminal protein and the DNA polymerase, *J. Virol. 61*, 3983−3991.
28. Truniger, V., Lazaro, J. M., Esteban, F. J., Blanco, L., and Salas, M. (2002) A positively charged residue of ϕ29 DNA polymerase, highly conserved in DNA polymerases from families A and B, is involved in binding the incoming nucleotide, *Nucleic Acids Res. 30*, 1483−1492.
29. Goodman, M. F., Keener, S., Guidotti, S., and Branscomb, E. W. (1983) On the enzymatic basis for mutagenesis by manganese, *J. Biol. Chem. 258*, 3469−3475.
30. Eigen, M. (1963) Fast Elementary Steps in Chemical Reaction Mechanisms, *Pure Appl. Chem. 6*, 97−115.
31. Margerun, D. W., Cayley, G. R., Watherburn, D. C., and Pagenkopf, G. K. (1978) in *Coordination Chemistry* (Martell, A. E., Ed.) American Chemical Society, Washington, DC.
32. Pelletier, H., and Sawaya, M. R. (1996) Characterization of the metal ion binding helix-hairpin-helix motifs in human DNA polymerase beta by X-ray structural analysis, *Biochemistry 35*, 12778−12787.
33. Pelletier, H., Sawaya, M. R., Wolfle, W., Wilson, S. H., and Kraut, J. (1996) A structural basis for metal ion mutagenicity and nucleotide selectivity in human DNA polymerase beta, *Biochemistry 35*, 12762−12777.
34. Yang, G., Franklin, M., Li, J., Lin, T. C., and Konigsberg, W. (2002) A conserved Tyr residue is required for sugar selectivity in a Pol alpha DNA polymerase, *Biochemistry 41*, 10256−10261.
35. Sarafianos, S. G., Clark, A. D., Jr., Das, K., Tuske, S., Birktoft, J. J., Ilankumaran, P., Ramesha, A. R., Sayer, J. M., Jerina, D. M., Boyer, P. L., Hughes, S. H., and Arnold, E. (2002) Structures of HIV-1 reverse transcriptase with pre- and post-translocation AZTMP-terminated DNA, *EMBO J. 21*, 6614−6624.
36. Florian, J., Goodman, M. F., and Warshel, A. (2003) Computer simulation of the chemical catalysis of DNA polymerases: discriminating between alternative nucleotide insertion mechanisms for T7 DNA polymerase, *J. Am. Chem. Soc. 125*, 8163−8177.
37. Florian, J., Goodman, M. F., and Warshel, A. (2003) Computer simulation studies of the fidelity of DNA polymerases, *Biopolymers 68*, 286−299.
38. Doublie, S., Tabor, S., Long, A. M., Richardson, C. C., and Ellenberger, T. (1998) Crystal structure of a bacteriophage T7 DNA replication complex at 2.2 Å resolution, *Nature 391*, 251−258.
39. Gangurde, R., Kaushik, N., Singh, K., and Modak, M. J. (2000) A carboxylate triad is essential for the polymerase activity of *Escherichia coli* DNA polymerase I (Klenow fragment). Presence of two functional triads at the catalytic center, *J. Biol. Chem. 275*, 19685−19692.
40. Arndt, J. W., Gong, W., Zhong, X., Showalter, A. K., Liu, J., Dunlap, C. A., Lin, Z., Paxson, C., Tsai, M. D., and Chan, M. K. (2001) Insight into the catalytic mechanism of DNA polymerase beta: structures of intermediate complexes, *Biochemistry 40*, 5368−5375.
41. Rittenhouse, R. C., Apostoluk, W. K., Miller, J. H., and Straatsma, T. P. (2003) Characterization of the active site of DNA polymerase beta by molecular dynamics and quantum chemical calculation, *Proteins 53*, 667−682.
42. Menge, K. L., Hostomsky, Z., Nodes, B. R., Hudson, G. O., Rahmati, S., Moomaw, E. W., Almassy, R. J., and Hostomska, Z. (1995) Structure−function analysis of the mammalian DNA polymerase beta active site: role of aspartic acid 256, arginine 254, and arginine 258 in nucleotidyl transfer, *Biochemistry 34*, 15934−15942.

BI049615P